Advanced Materials

Chromogenic Photonic Crystals Enabled by Novel Vapor-Responsive Shape Memory Polymers

--Manuscript Draft--

Manuscript Number:	adma.201500835
Full Title:	Chromogenic Photonic Crystals Enabled by Novel Vapor-Responsive Shape Memory Polymers
Article Type:	Communication
Section/Category:	
Keywords:	shape memory polymers; photonic crystals; macroporous; chromogenic; capillary condensation
Corresponding Author:	Peng Jiang University of Florida Gainesville, FL UNITED STATES
Additional Information:	
Question	**Response**
Please submit a plain text version of your cover letter here. **If you are submitting a revision of your manuscript, please do not overwrite your original cover letter. There is an opportunity for you to provide your responses to the reviewers later; please do not add them here**.	Dear Editor: Enclosed please find a manuscript entitled "Chromogenic Photonic Crystals Enabled by Novel Vapor-Responsive Shape Memory Polymers" by Y. Fang, Y. L. Ni, B. Choi, S. Y. Leo, J. Gao. B. Ge, C. Taylor, V. Basile and P. Jiang for consideration in Advanced Materials Communications. Smart shape memory polymers (SMPs) can memorize and recover their permanent shape in response to an external stimulus, such as heat, light, and solvent. They have been extensively exploited for a wide spectrum of applications ranging from biomedical devices (e.g., surgical stents and sutures) and implants for minimally invasive surgery to aerospace morphing structures and self-healing materials. However, most of the existing SMPs are thermoresponsive and their performance is hindered by slow response speed, heat-demanding programming and recovery steps. In this manuscript, by integrating scientific principles drawn from two disparate fields that do not typically intersect the fast-growing photonic crystal and SMP technologies, we report a new type of SMP that enables unusual "cold" programming and instantaneous shape recovery triggered by exposing the samples to various organic vapors. These stimuli-responsive materials differ greatly from existing SMPs as they enable orders of magnitude faster response, striking chromogenic effects, and room-temperature operations for the entire shape memory cycle, promising for many applications ranging from reusable chromogenic vapor sensors to reconfigurable nanooptical devices. Moreover, this interdisciplinary integration provides a simple and sensitive optical technique for investigating the intriguing shape memory effects at nanoscale. We believe this new type of smart material will be of interest to the diverse readership of Advanced Materials, such as researchers in the fields of photonic materials, sensors and actuators, polymers, and biomedical materials. We refer to a paper (Ref. 67) which is currently under revision at Nature Communications (with 2 minor revision requests), and enclose the paper for the review. We have also included 6 suggested reviewers and 1 exclude reviewer (due to possible conflict of interest). Thank you so much for your time in handling our manuscript. If you need any other information, please do not hesitate to contact me. Sincerely yours, Dr. Peng Jiang
Corresponding Author Secondary Information:	

Corresponding Author's Institution:	University of Florida
Corresponding Author's Secondary Institution:	
First Author:	Peng Jiang
First Author Secondary Information:	
Order of Authors:	Peng Jiang
	Yin Fang
	Yongliang Ni
	Baeck Choi
	Sin-Yen Leo
	Jian Gao
	Beverly Ge
	Curtis Taylor
	Vito Basile
Order of Authors Secondary Information:	
Abstract:	Smart shape memory polymers (SMPs) can memorize and recover their permanent shape in response to an external stimulus, such as heat, light, and solvent. They have been extensively exploited for a wide spectrum of applications ranging from biomedical devices (e.g., surgical stents and sutures) and implants for minimally invasive surgery to aerospace morphing structures and self-healing materials. However, most of the existing SMPs are thermoresponsive and their performance is hindered by slow response speed, heat-demanding programming and recovery steps. In this manuscript, by integrating scientific principles drawn from two disparate fields that do not typically intersect - the photonic crystal and SMP technologies, we report a new type of SMP that enables unusual "cold" programming and instantaneous shape recovery triggered by exposing the samples to various organic vapors. These stimuli-responsive materials differ greatly from existing SMPs as they enable orders of magnitude faster response, striking chromogenic effects, and room-temperature operations for the entire shape memory cycle, promising for many applications ranging from reusable chromogenic vapor sensors to reconfigurable nanooptical devices. Moreover, this interdisciplinary integration provides a simple yet sensitive optical technique for investigating the intriguing shape memory effects at nanoscale.

WILEY-VCH

DOI: 10.1002/((please add manuscript number))
Article type: Communication

Chromogenic Photonic Crystals Enabled by Novel Vapor-Responsive Shape Memory Polymers

*Yin Fang, Yongliang Ni, Baeck Choi, Sin-Yen, Leo, Jian Gao, Beverly Ge, Curtis Taylor, Vito Basile, and Peng Jiang**

Y. Fang, B. Choi, S. Y. Leo, J. Gao, B. Ge, Prof. P. Jiang
Department of Chemical Engineering, University of Florida, Gainesville, Florida 32611, USA
E-mail: pjiang@che.ufl.edu
Y. L. Ni, Prof. C. Taylor
Department of Mechanical and Aerospace Engineering, University of Florida, Gainesville, Florida 32611, USA
Dr. V. Basile
ITIA-CNR, Industrial Technologies and Automation Institute, National Council of Research, Via Bassini, 15, 20133 Milano, Italy

Keywords: shape memory polymers, photonic crystals, macroporous, chromogenic, capillary condensation

Shape memory polymers (SMPs) are a class of smart materials that can recover back to their "memorized" permanent shapes from temporary configurations in response to an external stimulus, such as heat, light, solvent, electric and magnetic fields.[1-12] Compared with their alloy counterparts (e.g., nitinol alloy), SMPs have gained increased attention due to their dramatically larger strain storage and recovery (up to 800% vs. less than 8%), light weight, low cost, ease of synthesis, and biocompatibility.[1,2,4-6,13] They have been extensively explored for a wide spectrum of technological applications, such as reconfigurable morphing structures,[14,15] smart textiles,[16,17] sensors and actuators,[18,19] self-healing materials,[20] surgical stents and sutures,[21,22] and implants for minimally invasive surgery.[23] Traditional thermoresponsive shape memory (SM) effect is usually achieved in three steps including programming, storage, and recovery.[6] Programming involves deforming a bulk SMP sample from its permanent shape to a temporary shape at a temperature higher than some specific transition temperatures (T_{trans}) of the polymer, such as melting temperature (T_m) or glass transition temperature (T_g). The deformed sample is then cooled below T_{trans} to fix the

temporary shape which can be stored at ambient conditions for a long period of time. Recovery to the permanent shape, which is caused by entropy elasticity, occurs when the sample is reheated to above T_{trans}.[5,6]

The recovery time for bulk thermoresponsive SMPs, which are mostly studied and employed in practical devices, is usually long.[5,6,13] This significantly impedes many applications that require fast response speed. Similar slow SM response is also suffered by many other types of SMPs activated through laser, solvent, electric field, infrared absorption and alternating magnetic field.[24-27] Indeed, most of these different SM activation mechanisms are still thermoresponsive as they depend on the generation of heat by various means to trigger the final shape recovery. Additionally, "hot" programming is generally utilized by almost every class of existing SMPs.[1-11,13,28,29] By contrast, SMPs that can be "cold" programmed (i.e., deformed to a temporary shape at or below room temperature), which could greatly enhance the processability to accommodate broader application requirements (e.g., room temperature operations for the entire SM cycle), are rare.[30,31] Moreover, most of the current SMP applications leverage the macroscopic SM effects and the deformation length scale is usually large (on the order of centimeter or larger). However, an intriguing potential for many new applications, largely unexplored, is the ability of SMPs to memorize and change shape at nanoscale.[32,33] Furthermore, although a variety of solvents (e.g., water) can trigger SM recovery by effectively reducing T_g of the polymer through the plasticizing effect,[34-39] vapor-responsive SMPs are uncommon.[40]

Here we report a new type of vapor-responsive SMP that enables unusual "cold" programming and instantaneous shape recovery at nanoscale. These novel SMPs were discovered in the fabrication of macroporous polymer photonic crystals. Photonic crystals are periodic dielectric structures with a forbidden gap (or photonic band gap) for electromagnetic waves, analogous to the electronic band gap in semiconductors which lies at the heart of microelectronics.[41-43] Photons with energies lying in the photonic band gap (PBG) cannot

propagate through the medium, providing unprecedented opportunities to control the flow of light in miniature volumes for a large variety of applications ranging from all-optical integrated circuits to diffractive optical devices (e.g., optical filters).[44,45] Tunable photonic crystals, whose lattice structures and PBGs can be adjusted by various stimuli, such as external pressure, electric and magnetic fields, solvents, vapors and metal ions, have been extensively investigated by using elastic materials (e.g., elastomers and gels).[46-64] However, the deformed photonic crystal structures cannot be memorized and they rapidly return to the original crystalline lattices once the external stimuli are released. Although smart SMPs could provide an unique opportunity to realize reconfigurable photonic crystals with bistable states (corresponding to the permanent and the temporary shapes of a SMP), these stimuli-responsive materials have rarely been used in previous photonic crystal studies.[65,66]

By integrating scientific principles drawn from two disparate fields that do not typically intersect – the fast-growing photonic crystal and SMP technologies, here we demonstrate that reconfigurable photonic crystals exhibiting striking chromogenic effects can be achieved by using a new type of vapor-responsive SMP. Interestingly, our recent work has shown that the SM recovery of the same type of SMP can also be rapidly triggered by applying an external contact pressure.[67] As illustrated by the scheme in **Figure 1**, the permanent photonic crystal configuration used in the current work is a three-dimensional (3-D) periodic array of macropores. These macroporous SMP photonic crystals were farbricated by using 3-D highly ordered silica colloidal crystals as structural templates.[68,69] The templating colloidal crystals were assembled by the convective self-assembly technology using silica microspheres with diameter ranging from 200 to 400 nm.[70] The thickness of the resulting colloidal crystal was controlled to ~ 3–5 μm (or ~ 10–20 colloidal monolayers) by adjusting the concentration of the colloidal suspensions in the convective self-assembly process. The interstitial air in-between the silica microspheres was replaced by viscous oligomer mixtures of ethoxylated (20) trimethylolpropane triacrylate (ETPTA 20, MW 1176,

viscosity 225 cps at 25 °C, T_g ~ –40 °C, refractive index ~ 1.470) and polyethylene glycol (600) diacrylate (PEGDA 600, MW 742, viscosity 90 cps at 25 °C, T_g ~ –42 °C, refractive index ~ 1.468) with varying volumetric ratios from 1:1 to 1:6. The molecular structures of these oligomers are shown in **Figure S1** in the Supporting Information. The oligomer mixture was then photocured at ambient conditions and the templating silica microspheres were selectively dissolved in a hydrofluoric acid aqueous solution, leaving behind a free-standing macroporous ETPTA 20-co-PEGDA 600 copolymer membrane with crystalline arrays of macropores. The size of the templated macropores, which determines the color of the final macroporous photonic crystal, is defined by the diameter of the templating silica microspheres. Differential scanning calorimetric (DSC) measurements (see a typical DSC plot of a macroporous ETPTA 20-co-PEGDA 600 copolymer film with 1:3 ratio in **Figure S2**) show the copolymers have T_g close to those of the two oligomer components (~ –42 °C), indicating the crosslinked copolymers are rubbery at room temperature. When immersed in water, the templated macroporous SMP membrane shows pale iridescent colors at large viewing angles (> 45 °) caused by Bragg diffraction of visible light from the periodic arrays of polymer macropores filled with water (refractive index 1.333). This confirms the maintenance of the 3-D ordered structure of the original silica colloidal crystal throughout the templating process.

The unusual "cold" programming process occurred when the macroporous SMP membrane dried out of water. Surprisingly, the iridescent color of the macroporous photonic crystal disappeared, and the film became translucent with a pale white appearance (**Figure 2**a). The typical cross-sectional scanning electron microscope (SEM) image of the water-dried sample in Figure 2b shows no apparent ordering of the templated macropores, indicating an order-disorder transition during water evaporation. The atomic force microscopy (AFM) image (Figure 2c) and the depth profile scanned across the line (Figure 2d) illustrate that the surface of the dried membrane is rough. The root-mean-square (RMS) linear profile

roughness (R_q) of the sample was determined to be 41.7 ± 7.8 nm (**Table 1**). We attributed this order-disorder transition during water evaporation to the large capillary pressure induced by the high surface tension of water (72.75 mN/m at 20 °C), which is sufficient to compress the ordered elastic macropores into disordered arrays. According to the Young-Laplace equation, $P_c = 2\gamma cos\theta / r$, the capillary pressure (P_c) is proportional to the liquid/vapor surface tension (γ) and $cos\theta$ (θ is the contact angle of the liquid on the pore surface); while inversely proportional to the radius of the pores (r).[71] Therefore, P_c can be reduced by using a solvent with a low surface tension (e.g., ethanol with γ ~ 22.39 mN/m at 20 °C), or by increasing the size of the pores. When P_c is small compared with the elastic modulus (or Young's modulus, E) of the copolymer membrane, we expect the templated SMP macropores will remain the original 3-D highly ordered structure, instead of being squeezed into disordered arrays. This speculation was supported by two experimental evidences. First, iridescent macroporous copolymer membranes with striking diffractive colors and much smoother surface (R_q ~ 7.7 ± 1.3 nm) resulted when the macroporous SMP samples dried out of ethanol instead of water. Second, our experiments showed that SMP membranes templated from large silica microspheres (> 600 nm) maintained the ordered structure even when dried out of water.

We evaluated the Young's modulus of the macroporous SMP membranes by *in-situ* nanoindentation tests. Three forces (100 μN, 200 μN, and 300 μN) were chosen to compare E of different indentation forces/depths. **Figure S3** shows the results of macroporous ETPTA 20-co-PEGDA 600 (1:3 ratio) membranes with 300 nm macropores dried out of ethanol and water, respectively. Apparently, all samples have Young's modulus of ~ 30 MPa, and the water-dried films are slightly stiffer than the ethanol-dried ones. This is reasonable as more air was trapped in the ethanol-dried samples with 3-D ordered macropores compared with the collapsed pores of the water-dried membranes. Similar E values were obtained from

macroporous copolymer samples with other oligomer volumetric ratios (from 1:1 to 1:6) and macropore sizes. By using the Young-Laplace equation, we estimated the capillary pressure generated by evaporating water from the copolymer macropores with 300 nm diameter to be ~ 1 MPa (i.e., ~ 10 atm), which is comparable with the Young's modulus of the macroporous SMP membranes. Similar capillary pressure-induced macropore collapse has been reported during drying of macroporous polymer (e.g., polysulfone) reverse osmosis membranes used for water purification.[72,73]

The autonomous evaporation-assisted "cold" programming exhibited by the macroporous SMP membranes is in sharp contrast to the common "hot" programming process used by traditional SMPs. Even more interesting, a translucent macroporous SMP copolymer membrane with collapsed macropores momentarily changed color from pale white to brilliant iridescence (**Figure 3**a) when the sample was exposed to various organic vapors (e.g., acetone, methanol, and chloroform) at ambient conditions (see **Video 1** in the Supporting Information). The cross-sectional SEM image in Figure 3b shows a SMP copolymer sample after exposing to an acetone vapor. The recovery of the 3-D highly ordered photonic crystal structure (permanent configuration) is evident. By averaging over 50 different spots on a few SEM images, the thickness of the macroporous layers of the water-dried and the acetone vapor-recovered SMP samples was estimated to be 1.95 ± 0.13 μm and 5.75 ± 0.06 μm, respectively. The nearly 3-fold expansion of the macroporous layer indicates the collapsed macropores popped up into ordered arrays when triggered by acetone vapor exposure. The AFM image and the depth profile in Figure 3c-d illustrate that the acetone-recovered macroporous SMP membrane has a much smoother surface than the water-dried sample (Figure 2c-d). Table 1 compares the surface roughness of a SMP membrane dried out water, ethanol, and acetone vapor. The acetone vapor-activated sample has a slightly rougher surface than the liquid ethanol-recovered one; while both samples are significantly smoother than the water-dried membrane.

The instantaneous transition between a disordered temporary configuration and a 3-D highly ordered permanent structure, which leads to an easily perceived color change from translucence to striking iridescence, can be quantitatively characterized by measuring the normal-incidence reflection spectra using an optical spectrometer. **Figure 4** compares the optical reflection spectra obtained from a water-dried SMP membrane with 280 nm macropores (black line), and the same sample after exposed to acetone vapor (red line) and liquid ethanol (blue line). No apparent Bragg diffraction peaks are shown in the spectrum of the water-dried sample; while distinct diffraction peaks with well-defined Fabry-Perot fringes are present in the spectra of the samples triggered by acetone vapor and liquid ethanol, confirming the high crystalline quality of the recovered macroporous photonic crystals.[69] Additionally, the experimental spectrum of the ethanol-recovered sample matches well with the calculated spectrum using a scalar-wave approximation (SWA) model, which assumes a perfect crystalline lattice.[74] We can then use the ethanol-activated SMP membrane as a fully recovered control to evaluate the completeness of macropore recovery under different triggering conditions. As shown in Figure 4, the amplitude of the PBG peaks of the acetone vapor-activated sample is slightly lower than that of the liquid ethanol-recovered one. As the PBG optical density of a macroporous photonic crystal is a sensitive function of its crystalline thickness,[74] the smaller reflection amplitude indicates the acetone vapor-triggered macropore recovery is not as complete as the liquid ethanol-induced recovery. This agrees with the surface roughness results shown in Table 1.

Above we have shown that the chromogenic responses enabled by the macroporous SMP photonic crystals with micrometer-scale thickness provide a simple yet sensitive optical methodology for characterizing microscopic SM effects. We then used this optical tool to evaluate the reversibility, durability, and reproducibility of the vapor-triggered SMP membranes. **Figure 5**a and 5b compare the optical reflection spectra obtained from the same macroporous ETPTA 20-co-PEGDA 600 (1:3 ratio) membrane cyclically exposed to acetone

vapor and then dried out of water for 10 times. The good reversibility and reproducibility of the sample are evident from the spectra and the comparison of the absolute reflection amplitude at 500 nm wavelength for the sample cyclically exposed to acetone vapor and water in Figure 5c. Indeed, our extensive tests showed that the macroporous SMP copolymer membranes could be reused for over 500 times without any apparent degradation in the chromogenic response to acetone vapor (see **Video 2** for a sample reused 2 times).

We speculated that the capillary condensation and evaporation of fluids with low surface tension in macroporous SMP membranes played a critical role in the vapor-triggered SM recovery.[71,75,76] As shown by Video 1 and **Figure 6**a-c, the translucent SMP membrane instantaneously changed color to reddish when the sample was close to the surface of liquid acetone, where the partial pressure of acetone vapor was high. Interestingly, the sample could become nearly transparent when it stayed close to the liquid acetone surface for a while. This indicates all macropores were filled up with condensed acetone whose refractive index (n_{acetone} ~ 1.359) is close to that of the ETPTA 20-co-PEGDA 600 copolymer (n_{copolym} ~ 1.470). The reddish color changed to greenish when the membrane moved away from the liquid acetone surface, and this red-green color transition was reversible (see Video 1). To gain quantitative insights into the capillary condensation of condensable vapors in the macroporous SMP membranes, we measured the normal-incidence optical reflection spectra for a sample with 300 nm macropores exposed to acetone vapors with different partial pressures (Figure 6d). The diffraction peak red-shifts with increasing vapor pressure, and it nearly disappears (due to refractive index matching) when the vapor partial pressure is very high (682.8 mmHg). We can calculate the effective refractive index (n_{eff}) of the macroporous photonic crystals with condensed liquid using the Bragg diffraction equation: $\lambda_{max} = 2 \times n_{eff} \times d \times \sin\theta$, where d is the inter-plane distance and θ is $\pi/2$ for normal incidence. By assuming the macropores are close-packed and the volume fraction of air (VF_{air}) in a dry macroporous SMP membrane is

0.74, we can then calculate the volume fraction of the condensed acetone ($VF_{acetone}$) using $n_{eff} = n_{copolym} \times 0.26 + n_{air} \times (0.74 - VF_{acetone}) + n_{acetone} \times VF_{acetone}$, where $n_{copolym}$, n_{air}, and $n_{acetone}$ is 1.47, 1.0, and 1.359, respectively. As shown in previous work,[75-77] the condensed liquid forms a uniform thin layer on the walls of the macropores. The thickness of this liquid layer and the size of the remaining air cavities can be easily evaluated by using $VF_{acetone}$. The calculated radius of air cavities for the 5 samples with apparent diffraction peaks and increasing vapor pressures in Figure 6d is 111.3, 99.8, 91.3, 81.9, sand 69.7 nm, respectively. We finally compared our experimental results with the predictions using the Kelvin equation, $ln\frac{P}{P_0} = -\frac{2\gamma V_l}{rRT}$, where P and P_0 are actual and saturation vapor pressure, γ is the liquid/vapor surface tension, V_l is the liquid molar volume, r is the radius of curvature.[75] The Kelvin equation has been widely utilized in describing the phenomenon of capillary condensation due to the presence of a curved meniscus. It predicts *lnP* is linearly proportional to *1/r* when other variables are constant. Our experimental results match well with this prediction (inset of Figure 6d).

The overall shape memory cycle enabled by the novel vapor-responsive SMPs can be summarized as follows. When photopolymerized in the presence of the silica colloidal crystal template, the cross-linked polymer chains are in stress-free configurations which are energetically favorable. The large capillary pressure induced by the evaporation of water trapped in the templated macropores squeezes the 3-D ordered macropores into temporary disordered arrays. Excess stresses are stored in the deformed polymer chains and they tend to recover back to the original stress-free state due to entropy elasticity. The rapid capillary condensation of acetone vapors in the macropores triggers the instantaneous recovery of the permanent photonic crystal structure. As the surface tensions of the condensed liquids (e.g., acetone and methanol) are significantly lower than that of water, the evaporation-induced

capillary pressure is not sufficient to deform the recovered macropores during capillary evaporation of the condensed liquids.

In conclusion, we have discovered a new type of vapor-responsive SMP that enables room-temperature operations for the entire shape memory cycle. The recovery of the permanent macroporous photonic crystal structure can be momentarily triggered by a variety of organic vapors. The striking chromogenic effect (from colorless to iridescent) induced by the disorder-order transition differs greatly from the typical color change with limited wavelength shift exhibited by traditional tunable photonic crystals. In addition, the thin photonic crystal structure provides a simple yet sensitive optical technique for investigating the intriguing SM effects at nanoscale. These smart stimuli-responsive materials could find important technological applications ranging from reconfigurable nanooptical devices to reusable chromogenic vapor sensors.

Experimental Section

Fabrication of macroporous SMP photonic crystal membranes: The synthesis of monodispersed silica microspheres with less than 5% diameter variation was performed by following the well-established Stöber method.[78] The synthesized silica microspheres were purified in 200-proof ethanol by multiple (at least 6 times) centrifugation and redispersion cycles. The purified silica particles were then assembled into 3-D highly ordered colloidal crystals on glass microslides using the convective self-assembly technology.[70] The microslide with the silica colloidal crystal on its surface was covered by another microslide, separated by a double-sided adhesive tape spacer (~ 1.7 mm thick). By utilizing capillary force, the interstitials in-between the assembled silica microspheres were filled up with viscous oligomer mixtures consisting of ethoxylated (20) trimethylolpropane triacrylate (SR415, Sartomer) and polyethylene glycol (600) diacrylate (SR610, Sartomer) oligomers with varying volumetric ratios from 1:1 to 1:6. Darocur 1173 (2-hydroxy-2-methyl-1-phenyl-

1-propanone, BASF, 1 wt %) was added as photoinitiator. The monomer mixture was photopolymerized by using a pulsed UV curing system (RC 742, Xenon) for 4 s. The solidified film was soaked in a 1 vol % hydrofluoric acid aqueous solution for 4 h and finally rinsed with deionized water.

Responses of macroporous SMP membranes exposed to acetone vapors with different partial pressures: The templated macroporous SMP photonic crystal membrane was placed horizontally in a home-made environmental chamber.[77] A reflection probe (R600-7, Ocean Optics) connected to an Ocean Optics HR4000 high-resolution vis-NIR spectrometer was sealed in the environmental chamber to measure the optical reflectance from the SMP photonic crystal. The chamber was first purged with pure nitrogen gas for 2 min. It was then filled up with acetone vapors with different pressures. Dry nitrogen was used to control the total pressure of the chamber to 1 atm.

Sample characterization: SEM imaging was carried out on a FEI XL-40 FEG-SEM. A 15 nm thick gold layer was sputtered onto the samples prior to imaging. Amplitude-modulation atomic force microscopy (AM-AFM) was performed uing a MFP-3D AFM (Asylum Research, Inc.) with a Nanosensor PPP-NCHR probe (tip radius < 10 nm). Differential scanning calorimetric measurements were performed from –80 to 18 °C at a heating rate of 10 °C min^{-1} using a Seiko DSC 6200 instrument and an empty pan as reference. Normal-incidence optical reflection spectra were obtained using the Ocean Optics HR4000 high-resolution vis-NIR spectrometer with the R600-7 reflection probe and a tungsten halogen light source (LS-1). Absolute reflectivity was obtained as the ratio of the sample spectrum and a reference spectrum, which was the optical density obtained from an aluminum-sputtered (1000 nm thick) silicon wafer.

Nanoindentation tests: Nanoindentation tests were performed with a MFP-3D Nanoindenter (Asylum Research, Inc.) using a spherical sapphire indenter (tip radius ~ 125 μm). Such configuration of the instrument has a force and displacement resolution less than 3 μN and 1

nm, respectively. Due to the comparatively large contact area of the spherical tip, there is no need to perform a contact area calibration. A force controlled trapezoidal load function with a 5-2-2 seconds segments corresponding to loading-hold-unloading times was applied to all indentations. Three forces, 100 μN, 200 μN, and 300 μN, were chosen to compare the Young's modulus of different indentation forces/depths. With each force, ten impressions were indented on each sample with an inter-distance of 200 μm, which is about ten times over the average residual impression size. All indentations were triggered by 7.5 μN force, corresponding to ~ 2 nm deflection in the indenter spring. Overall, 30 indents were made on each sample. All indents were made at room temperature (23 °C) and the system was allowed to reach thermal equilibrium for 30 minutes to minimize the thermal drift effect.

Scalar wave approximation modeling: The scalar wave theory developed for periodic dielectric structures, which solves Maxwell's equations by neglecting diffraction from all but one set of crystalline planes (e.g., the (111) planes in this study),[74] was utilized to calculate the normal-incidence optical reflection spectra from macroporous SMP photonic crystals. The structural parameters of the photonic crystals used in the optical modeling, including the size of the macropores and the crystalline thickness, were derived from SEM images. The refractive index of the SMP copolymers was assumed to be 1.47.

Supporting Information

Supporting Information is available from the Wiley Online Library or from the author.

Acknowledgements

Acknowledgments are made to the US Defense Threat Reduction Agency (DTRA) under Contract No. HDTRA1-15-1-0022, US National Aeronautics and Space Administration (NASA) under Grant Award No. NNX14AB07G, and US National Science Foundation (NSF) under Award No. CMMI-1300613.

Received: ((will be filled in by the editorial staff))
Revised: ((will be filled in by the editorial staff))
Published online: ((will be filled in by the editorial staff))

[1] A. Lendlein, Ed. *Shape Memory Polymers*, Springer, New York, NY 2010.

[2] W. M. Huang, B. Yang, Y. Q. Fu, *Polyurethane Shape Memory Polymers*, CRC Press, Boca Raton, FL 2012.

[3] D. Habault, H. Zhang, Y. Zhao, *Chem. Soc. Rev.* **2013**, *42*, 7244.

[4] C. Yakacki, K. Gall, *Adv. Polym. Sci.* **2010**, *226*, 147.

[5] T. Xie, *Polymer* **2011**, *52*, 4985.

[6] A. Lendlein, S. Kelch, *Angew. Chem. Int. Ed.* **2002**, *41*, 2034.

[7] C. Liu, H. Qin, P. T. Mather, *J. Mater. Chem.* **2007**, *17*, 1543.

[8] H. Meng, J. Hu, *J. Intel. Mater. Syst. Str.* **2010**, *21*, 859.

[9] T. D. Nguyen, C. M. Yakacki, P. D. Brahmbhatt, M. L. Chambers, *Adv. Mater.* **2010**, *22*, 3411.

[10] M. A. C. Stuart, W. T. S. Huck, J. Genzer, M. Mueller, C. Ober, M. Stamm, G. B. Sukhorukov, I. Szleifer, V. V. Tsukruk, M. Urban, F. Winnik, S. Zauscher, I. Luzinov, S. Minko, *Nature Mater.* **2010**, *9*, 101.

[11] C. M. Yakacki, *Polym. Rev.* **2013**, *53*, 1.

[12] C. J. Kloxin, C. N. Bowman, *Chem. Soc. Rev.* **2013**, *42*, 7161.

[13] M. Behl, M. Y. Razzaq, A. Lendlein, *Adv. Mater.* **2010**, *22*, 3388.

[14] L. Ionov, *Polym. Rev.* **2013**, *53*, 92.

[15] S. M. Felton, M. T. Tolley, B. Shin, C. D. Onal, E. D. Demaine, D. Rus, R. J. Wood, *Soft Matter* **2013**, *9*, 7688.

[16] A. Gugliuzza, E. Drioli, *J. Membr. Sci.* **2013**, *446*, 350.

[17] J. Leng, H. Lu, Y. Liu, W. M. Huang, S. Du, *MRS Bull.* **2009**, *34*, 848.

[18] M. F. Metzger, T. S. Wilson, D. Schumann, D. L. Matthews, D. J. Maitland, *Biomed. Microdevices* **2002**, *4*, 89.

[19] W. Small, T. S. Wilson, W. J. Benett, J. M. Loge, D. J. Maitland, *Opt. Express* **2005**, *13*, 8204.

[20] H. Tobushi, H. Hara, E. Yamada, S. Hayashi, *Smart Mater. Struct.* **1996**, *5*, 483.

[21] A. Lendlein, R. Langer, *Science* **2002**, *296*, 1673.

[22] L. Xue, S. Dai, Z. Li, *J. Mater. Chem.* **2012**, *22*, 7403.

[23] C. M. Yakacki, R. Shandas, C. Lanning, B. Rech, A. Eckstein, K. Gall, *Biomaterials* **2007**, *28*, 2255.

[24] D. J. Maitland, M. F. Metzger, D. Schumann, A. Lee, T. S. Wilson, *Laser Surg. Med.* **2002**, *30*, 1.

[25] J. Leng, H. Lv, Y. Liu, S. Du, *J. Appl. Phys.* **2008**, *104*, 104917.

[26] H. Koerner, G. Price, N. A. Pearce, M. Alexander, R. A. Vaia, *Nature Mater.* **2004**, *3*, 115.

[27] C. S. Hazelton, S. C. Arzberger, M. S. Lake, N. A. Munshi, *J. Adv. Mater.* **2007**, *39*, 35.

[28] H. Meng, H. Mohamadian, M. Stubblefield, D. Jerro, S. Ibekwe, S.-S. Pang, G. Li, *Smart Mater. Struct.* **2013**, *22*.

[29] P. T. Mather, X. Luo, I. A. Rousseau, *Annu. Rev. Mater. Res.*, Vol. 39, 2009, 445.

[30] B. Heuwers, A. Beckel, A. Krieger, F. Katzenberg, J. C. Tiller, *Macromol. Chem. Phys.* **2013**, *214*, 912.

[31] B. Heuwers, D. Quitmann, R. Hoeher, F. M. Reinders, S. Tiemeyer, C. Sternemann, M. Tolan, F. Katzenberg, J. C. Tiller, *Macromol. Chem. Phys.* **2013**, *34*, 180.

[32] T. Xie, X. Xiao, J. Li, R. Wang, *Adv. Mater.* **2010**, *22*, 4390.

[33] H. Xu, C. Yu, S. Wang, V. Malyarchuk, T. Xie, J. A. Rogers, *Adv. Funct. Mater.* **2013**, *23*, 3299.

[34] J. Kunzelman, T. Chung, P. T. Mather, C. Weder, *J. Mater. Chem.* **2008**, *18*, 1082.

[35] H. Lv, J. Leng, Y. Liu, S. Du, *Adv. Eng. Mater.* **2008**, *10*, 592.

[36] W. M. Huang, B. Yang, L. An, C. Li, Y. S. Chan, *Appl. Phys. Lett.* **2005**, *86*, 114105.

[37] H. Du, J. Zhang, *Soft Matter* **2010**, *6*, 3370.

[38] X. Gu, P. T. Mather, *RSC Adv.* **2013**, *3*, 15783.

[39] D. Quitmann, N. Gushterov, G. Sadowski, F. Katzenberg, J. C. Tiller, *Adv. Mater.* **2014**, *26*, 3441.

[40] X. M. Ding, J. L. Hu, X. M. Tao, C. P. Hu, G. Y. Wang, *J. Appl. Polym. Sci.* **2008**, *107*, 4061.

[41] J. D. Joannopoulos, R. D. Meade, J. N. Winn, *Photonic Crystals: Molding the Flow of Light*, Princeton University Press, Princeton 1995.

[42] C. Fenzl, T. Hirsch, O. S. Wolfbeis, *Angew. Chem. Int. Ed.* **2015**, *53*, 3318.

[43] B. Hatton, L. Mishchenko, S. Davis, K. H. Sandhage, J. Aizenberg, *Proc. Natl. Acad. Sci. USA* **2010**, *107*, 10354.

[44] Y. A. Vlasov, X. Z. Bo, J. C. Sturm, D. J. Norris, *Nature* **2001**, *414*, 289.

[45] J. M. Weissman, H. B. Sunkara, A. S. Tse, S. A. Asher, *Science* **1996**, *274*, 959.

[46] A. C. Arsenault, T. J. Clark, G. Von Freymann, L. Cademartiri, R. Sapienza, J. Bertolotti, E. Vekris, S. Wong, V. Kitaev, I. Manners, R. Z. Wang, S. John, D. Wiersma, G. A. Ozin, *Nature Mater.* **2006**, *5*, 179.

[47] C. I. Aguirre, E. Reguera, A. Stein, *Adv. Funct. Mater.* **2010**, *20*, 2565.

[48] Y. Kang, J. J. Walish, T. Gorishnyy, E. L. Thomas, *Nature Mater.* **2007**, *6*, 957.

[49] H. Fudouzi, Y. N. Xia, *Langmuir* **2003**, *19*, 9653.

[50] J. Ge, J. Goebl, L. He, Z. Lu, Y. Yin, *Adv. Mater.* **2009**, *21*, 4259.

[51] J.-H. Jang, C. Y. Koh, K. Bertoldi, M. C. Boyce, E. L. Thomas, *Nano Lett.* **2009**, *9*, 2113.

[52] Y. Takeoka, M. Watanabe, *Langmuir* **2002**, *18*, 5977.

[53] J. Ge, Y. Hu, Y. Yin, *Angew. Chem. Int. Ed.* **2007**, *46*, 7428.

[54] E. P. Chan, J. J. Walish, A. M. Urbas, E. L. Thomas, *Adv. Mater.* **2013**, *25*, 3934.

[55] Z. Pan, J. Ma, J. Yan, M. Zhou, J. Gao, *J. Mater. Chem.* **2012**, *22*, 2018.

[56] I. B. Burgess, M. Loncar, J. Aizenberg, *J. Mater. Chem. C* **2013**, *1*, 6075.

[57] Y. Yue, T. Kurokawa, M. A. Haque, T. Nakajima, T. Nonoyama, X. Li, I. Kajiwara, J. P. Gong, *Nature Commun.* **2014**, *5*.

[58] Y. F. Yue, M. A. Haque, T. Kurokawa, T. Nakajima, J. P. Gong, *Adv. Mater.* **2013**, *25*, 3106.

[59] J. Cui, W. Zhu, N. Gao, J. Li, H. Yang, Y. Jiang, P. Seidel, B. J. Ravoo, G. Li, *Angew. Chem. Int. Ed.* **2014**, *53*, 3844.

[60] M. G. Han, C. G. Shin, S.-J. Jeon, H. Shim, C.-J. Heo, H. Jin, J. W. Kim, S. Lee, *Adv. Mater.* **2012**, *24*, 6438.

[61] D. Yang, S. Ye, J. Ge, *Adv. Funct. Mater.* **2014**, *24*, 3197.

[62] S. Ye, Q. Fu, J. Ge, *Adv. Funct. Mater.* **2014**, *24*, 6430.

[63] S. A. Asher, V. L. Alexeev, A. V. Goponenko, A. C. Sharma, I. K. Lednev, C. S. Wilcox, D. N. Finegold, *J. Am. Chem. Soc.* **2003**, *125*, 3322.

[64] J. H. Holtz, S. A. Asher, *Nature* **1997**, *389*, 829.

[65] C. G. Schaefer, M. Gallei, J. T. Zahn, J. Engelhardt, G. P. Hellmann, M. Rehahn, *Chem. Mater.* **2013**, *25*, 2309.

[66] C. G. Schaefer, D. A. Smolin, G. P. Hellmann, M. Gallei, *Langmuir* **2013**, *29*, 11275.

[67] Y. Fang, Y. L. Ni, S. Y. Leo, C. Taylor, V. Basile, P. Jiang, *Nature Commun.* **2015**, under revision.

[68] O. D. Velev, T. A. Jede, R. F. Lobo, A. M. Lenhoff, *Nature* **1997**, *389*, 447.

[69] P. Jiang, K. S. Hwang, D. M. Mittleman, J. F. Bertone, V. L. Colvin, *J. Am. Chem. Soc.* **1999**, *121*, 11630.

[70] P. Jiang, J. F. Bertone, K. S. Hwang, V. L. Colvin, *Chem. Mater.* **1999**, *11*, 2132.

[71] S. J. Gregg, K. S. W. Sing, *Adsorption, Surface Area and Porosity*, Academic Press Inc., London 1982.

[72] J. T. Tsai, Y. S. Su, D. M. Wang, J. L. Kuo, J. Y. Lai, A. Deratani, *J. Membr. Sci.* **2010**, *362*, 360.

[73] M. D. Mason, D. J. Sirbuly, S. K. Buratto, *Thin Solid Films* **2002**, *406*, 151.

[74] J. F. Bertone, P. Jiang, K. S. Hwang, D. M. Mittleman, V. L. Colvin, *Phys. Rev. Lett.* **1999**, *83*, 300.

[75] Z. Gemici, P. I. Schwachulla, E. H. Williamson, M. F. Rubner, R. E. Cohen, *Nano Lett.* **2009**, *9*, 1064.

[76] R. A. Potyrailo, H. Ghiradella, A. Vertiatchikh, K. Dovidenko, J. R. Cournoyer, E. Olson, *Nature Photon.* **2007**, *1*, 123.

[77] H. T. Yang, P. Jiang, *Appl. Phys. Lett.* **2011**, *98*, 011104.

[78] W. Stober, A. Fink, E. Bohn, *J. Colloid Interf. Sci.* **1968**, *26*, 62.

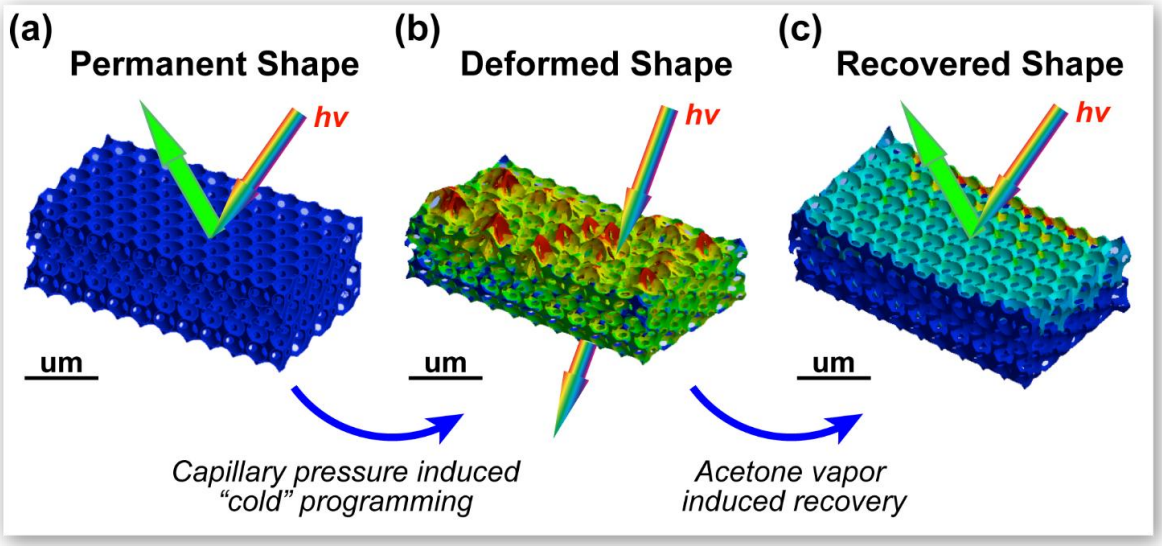

Figure 1. Schematic illustration showing the SM effects of the new vapor-responsive SMP. a) Thin macroporous SMP photonic crystal with 3-D ordered structure can diffract light with specific wavelengths. b) The unusual "cold" programming process deforms the ordered macropores into disordered array with rough surface and no light diffraction. c) The recovery of the permanent photonic crystal structure can be triggered by exposing the deformed membrane to various organic vapors (e.g., acetone).

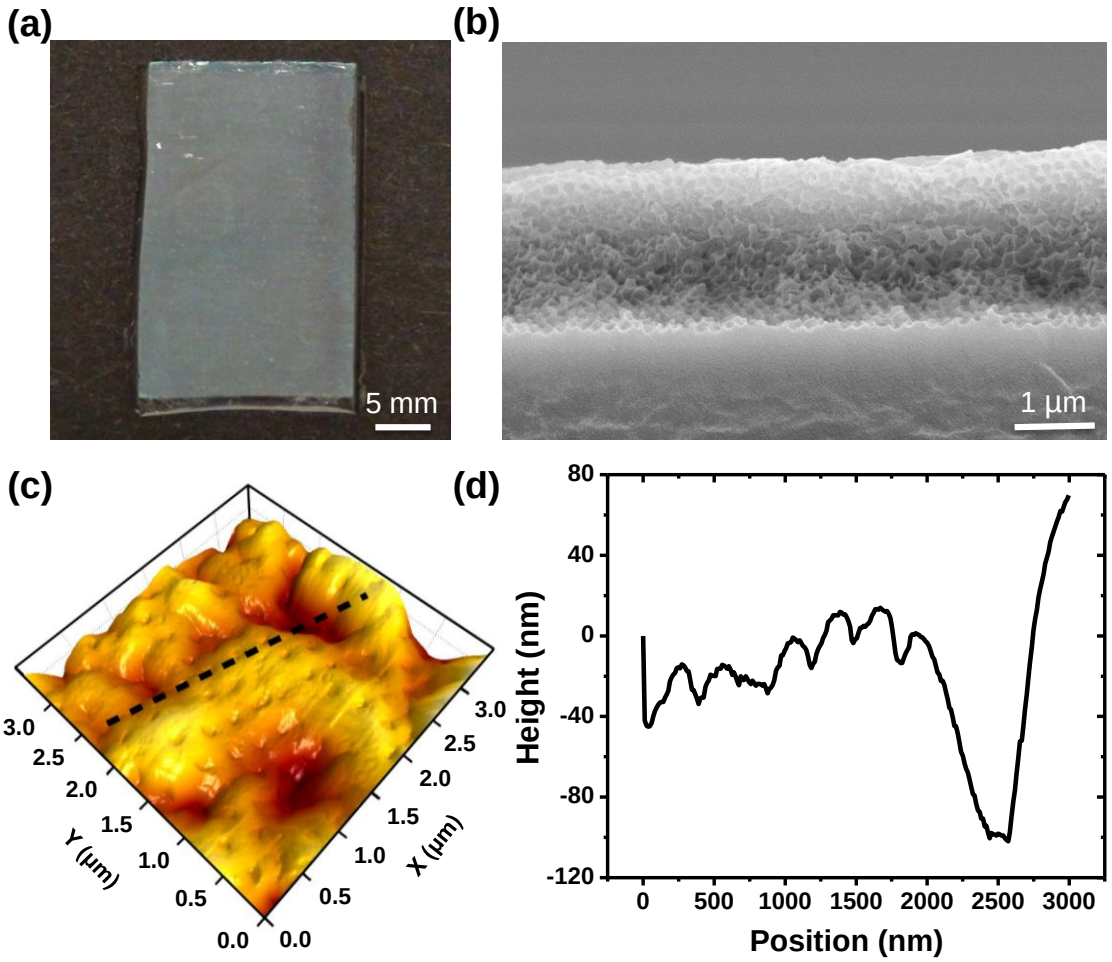

Figure 2. a) Photograph of a macroporous SMP membrane with 280 nm macropores after drying out of water. b) Cross-sectional SEM image of the sample. c) AFM scan of the sample surface. d) Height profile of the dashed line in c).

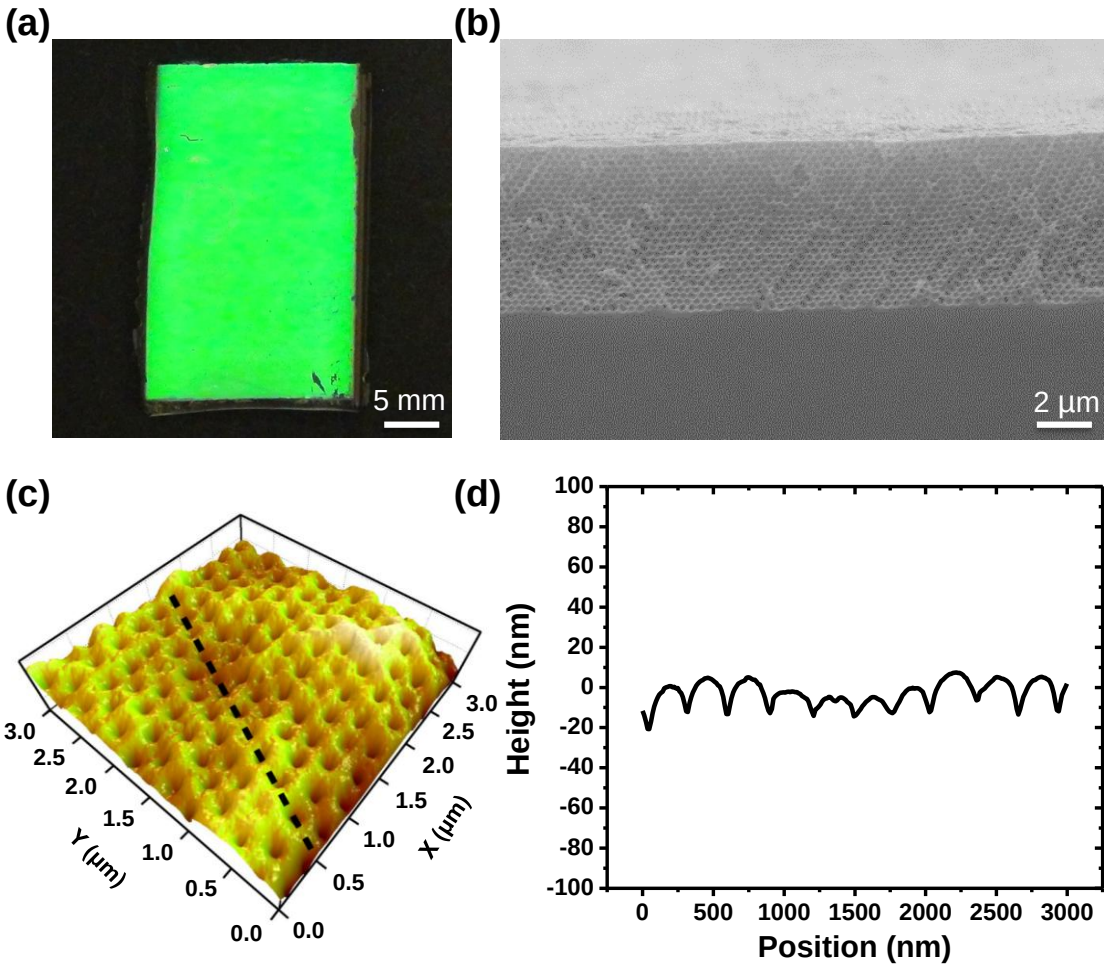

Figure 3. a) Photograph of a macroporous SMP membrane with 280 nm macropores after exposing to an acetone vapor. b) Cross-sectional SEM image of the sample. c) AFM scan of the sample surface. d) Height profile of the dashed line in c).

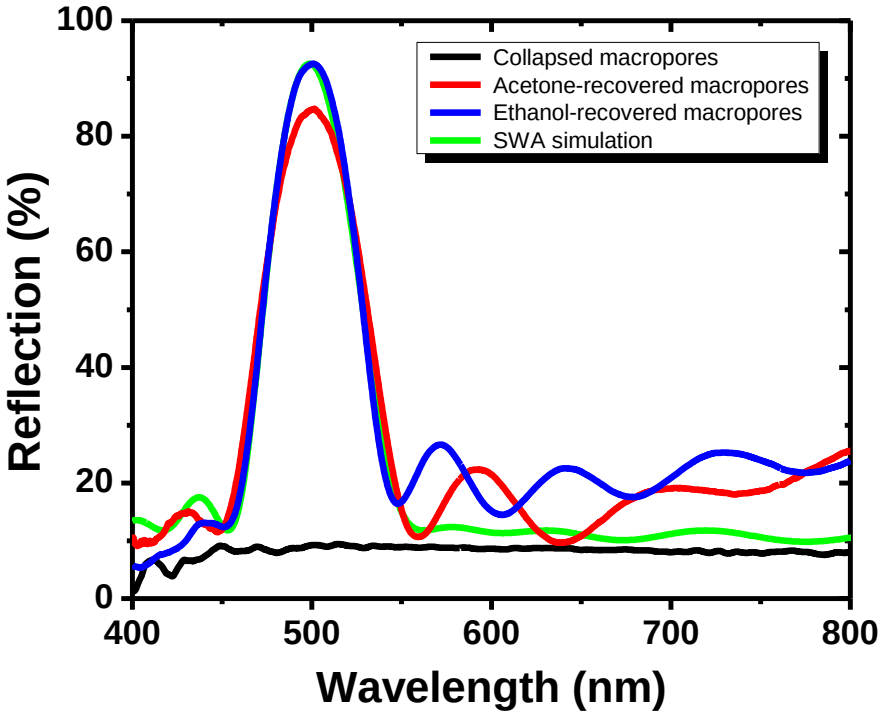

Figure 4. Normal-incidence optical reflection spectra comparing a macroporous SMP membrane with 280 nm macropores dried out of water, liquid ethanol, and acetone vapor. The calculated spectrum using a SWA model is also shown to compare with the experimental results.

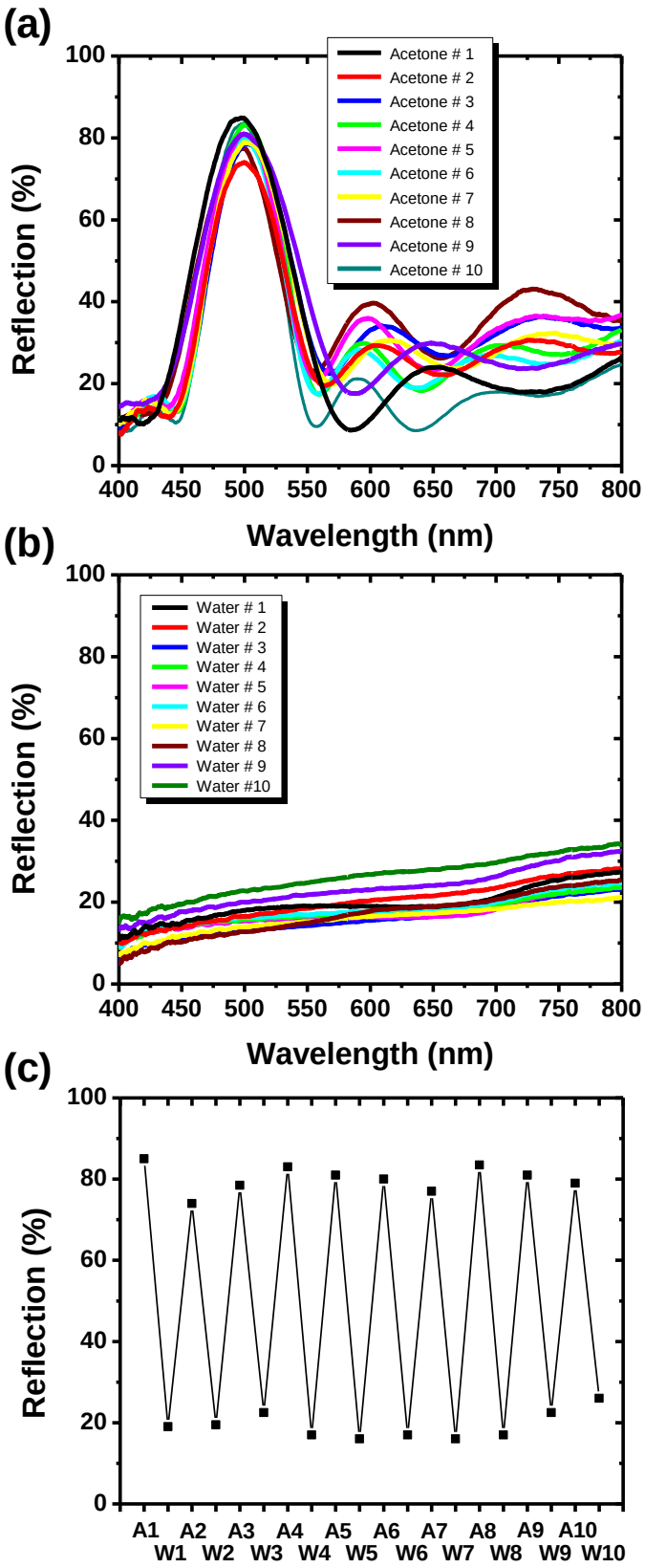

Figure 5. a) Normal-incidence optical reflection spectra obtained from a macroporous SMP membrane with 280 nm macropores exposed to acetone vapor for 10 times. b) Normal-incidence reflection spectra of the same sample after drying out of water for 10 times. c) Reflection amplitudes of the spectra in a) and b) taken at 500 nm wavelength.

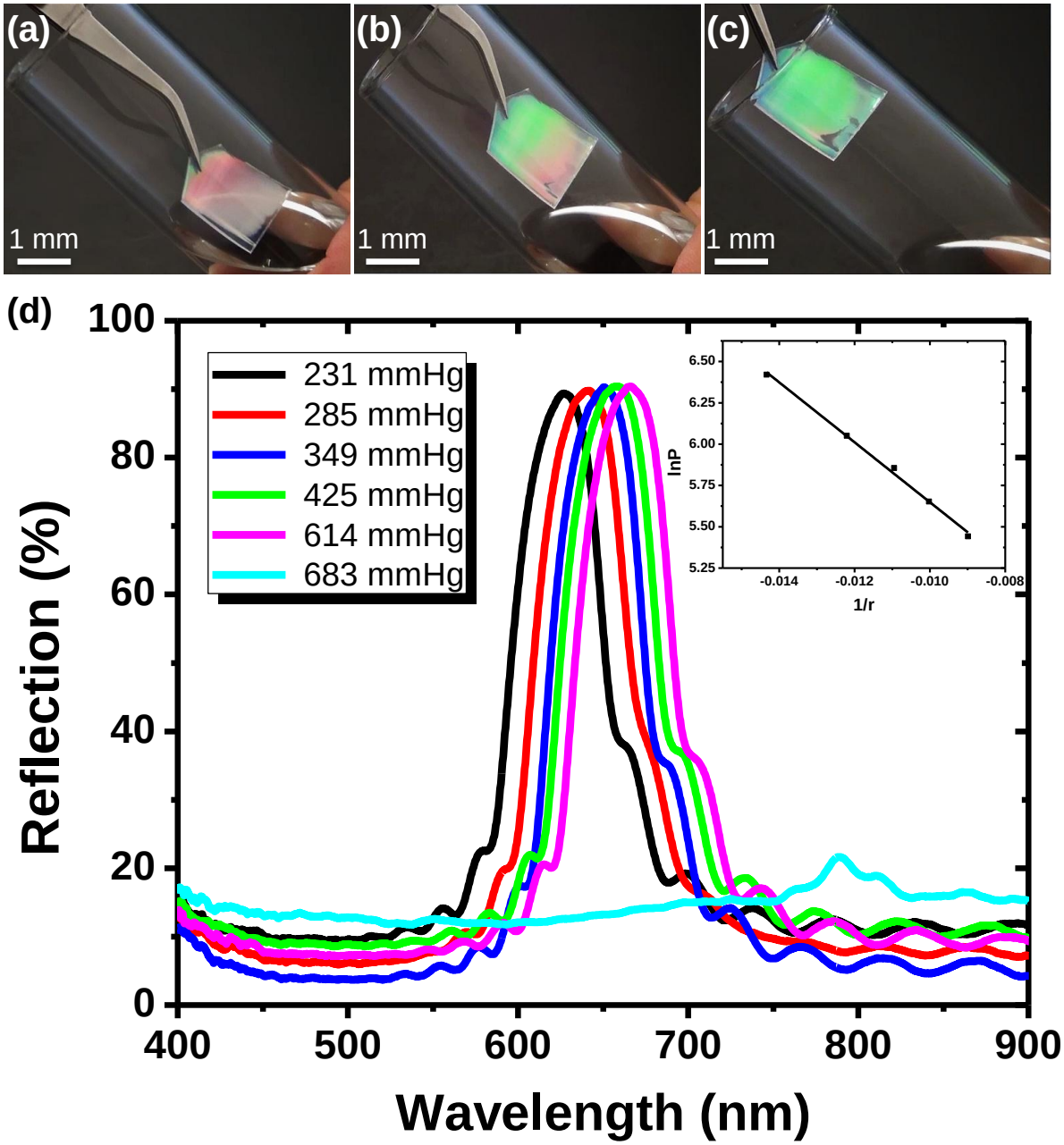

Figure 6. a-c) Photographs showing a macroporous SMP membrane exposed to acetone vapor above liquid acetone at different locations. d) Normal-incidence optical reflection spectra obtained from a macroporous SMP membrane exposed to acetone vapors with different partial pressures. Inset showing dependence of lnP vs the reciprocal of the radius of curvature of the condensed acetone films. The pressure is in unit of mmHg and the radius of curvature is in unit of nm.

Table 1. Roughness of 10 × 10 μm^2 AFM scan area of SMP sample surface.

Samples	3-D Areal Roughness		Linear Profile Roughness	
	AA Roughness, S_a [nm]	RMS Roughness, S_q [nm]	AA Roughness, R_a [nm]	RMS Roughness, R_q [nm]
Water-dried	46.5 ± 7.1	59.4 ± 9.9	34.6 ± 6.3	41.7 ± 7.8
Liquid ethanol-activated	8.7 ± 2.5	11.9 ± 4.3	6.3 ± 1.2	7.7 ± 1.3
Acetone vapor-activated	10.2 ± 1.6	14.0 ± 2.6	7.2 ± 1.1	8.9 ± 1.2

By integrating scientific principles drawn from two disparate fields – the fast-growing photonic crystal and shape memory polymer (SMP) technologies, we discovered a new type of SMP that enables room-temperature operations for the entire shape memory cycle and instantaneous shape recovery triggered by exposure to a variety of organic vapors.

Keyword: shape memory polymers, photonic crystals, macroporous, chromogenic, capillary condensation

Y. Fang, Y. L. Ni, B. Choi, S. Y. Leo, J. Gao, B. Ge, C. Taylor, V. Basil, P. Jiang*

Chromogenic Photonic Crystals Enabled by Novel Vapor-Responsive Shape Memory Polymers

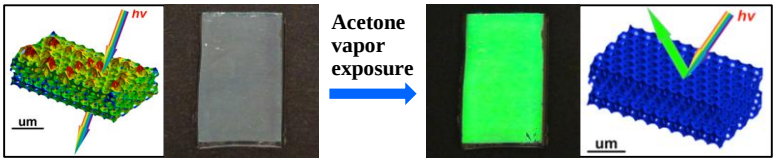

Supporting Information

Chromogenic Photonic Crystals Enabled by Novel Vapor-Responsive Shape Memory Polymers

*Yin Fang, Yongliang Ni, Baeck Choi, Sin-Yen, Leo, Jian Gao, Beverly Ge, Curtis Taylor, Vito Basile, and Peng Jiang**

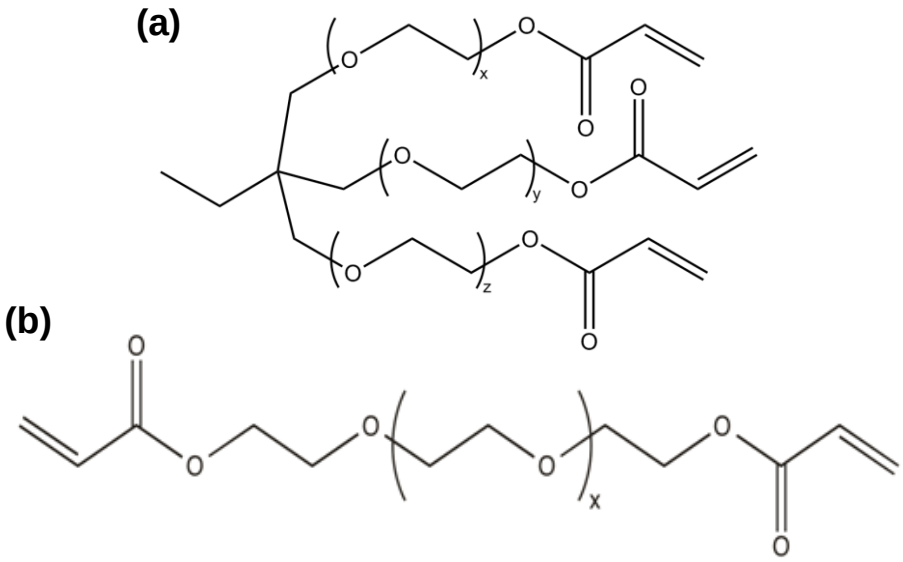

Figure S1. a) Molecular structure of ETPTA 20 (x + y + z = 20). b) Molecular structure of PEGDA 600 (x = 12).

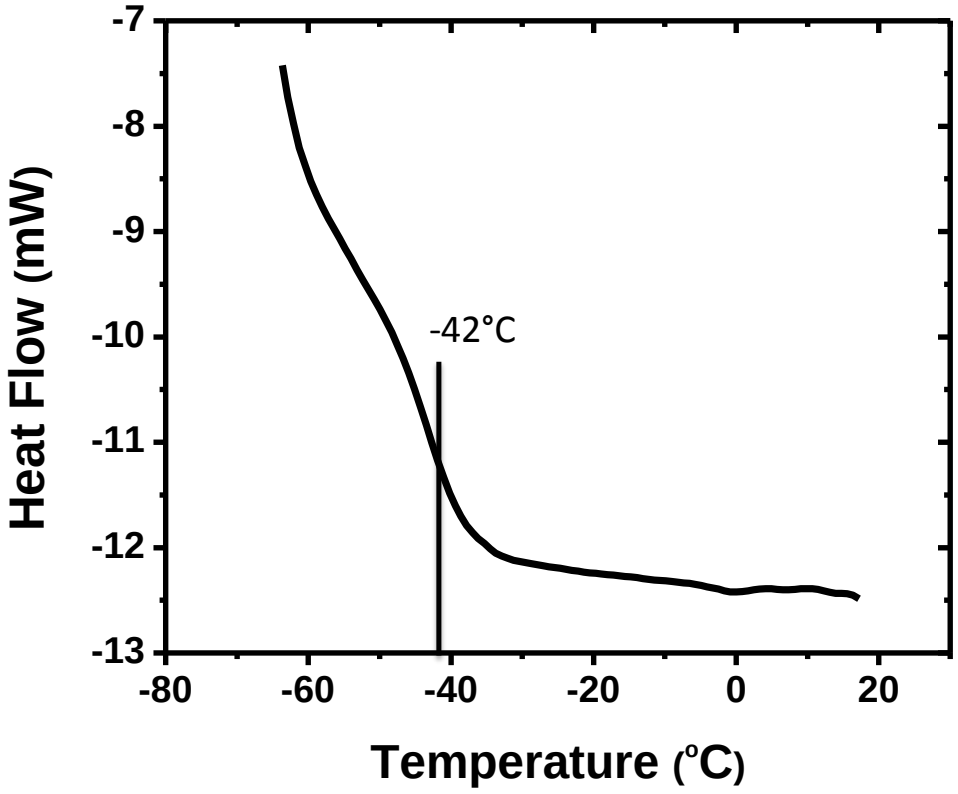

Figure S2. Typical DSC plot of a macroporous ETPTA 20-co-PEGDA 600 copolymer with 1:3 ratio.

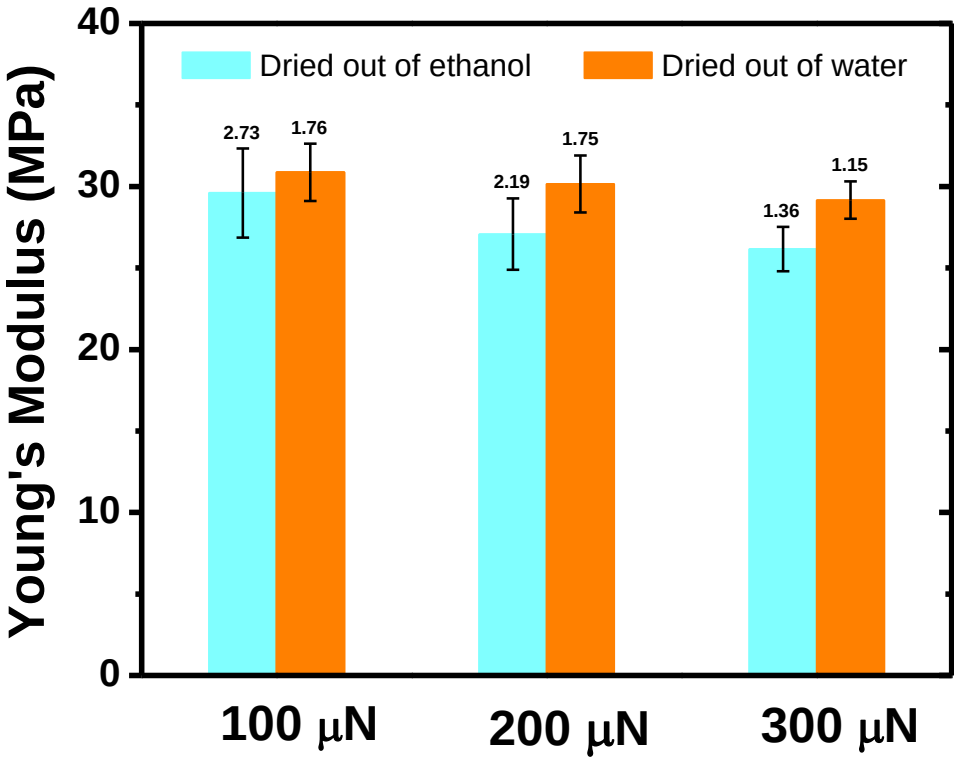

Figure S3. Comparison of the Young's modulus of the ethanol-dried and water-dried macroporous ETPTA 20-co-PEGDA 600 (1:3 ratio) membranes indented with different forces.

Video 1
Click here to download Supporting Information: Acetone Trigger Original.mp4

Video 2

Click here to download Supporting Information: Re-use.mp4

Supporting Information

Click here to download Supporting Information: Manuscript.pdf